Journal of Natural Sciences and Mathematics Research
J. Nat. Scien. & Math. Res. Vol. 10 No. 1 (2024) 93-105
ISSN: 2460-4453 (Online); 2614-6487 (Printed)
Available online at http://journal.walisongo.ac.id/index.php/jnsmr

Effect of chemical absorption on Jeffery Fluid Flow in saturated Porous Media with variable thermal conductivity

Akeem Babatunde Disu[1], Emmanuel Omokhuale[2], and Sulyman Olakunle Salawu[3]

[1]Department of Mathematics, National Open University of Nigeria, Nigeria
[2]Department of Mathematical Sciences, Federal University Gusau, Nigeria
[3]Department of Mathematics, Bowen University, Nigeria

Corresponding author's e-mail: adisu@noun.edu.ng

ABSTRACT

This study investigates the impact of species absorption of Jeffery fluid flow through a saturated permeable medium with variable thermal conductivity. The dimensional partial nonlinear derivative model controlling the chemical reacting fluid flow is transformed to invariant form. The resulting flow equations are computed numerically using an approximated finite implicit Crack-Nicolson. A chemical absorption of fluid reactant occurs in a boundless vertical device. Computations are performed for different parameters to examine their sensitivity under isothermal temperature conditions. The computed results are offered graphically for qualitative and quantitative insights into the flow behaviour. The obtained outcomes revealed that the fluid flow rate rises with an increasing values of the parameters $Gr, Gc, S, Da, \phi, \eta$ and λ_1, and it damps with upsurge in the values of the parameters Pr, Sc, M, Fs, γ, Ec and R. The heat transfer field is reduced with enhancing values of the thermal source, viscous dissipation and time, but declines for a boosted value of the terms suction and Prandtl number. Also, the mass transfer field is higher when mass absorption and time are increased, and diminish with an elevate in the values of Schmidt number and chemical reactions.

Keywords:
Thermal conductivity; Heat and mass diffusion; Porous medium; Jeffery material; Finite difference method.

Introduction

In the presence of chemically reacting fluid species, the combination of thermal and mass propagation is highly essential in several chemical processes. As such, a reasonable time has been devoted to it by many scholars owing to its industrial applications in drying processes, temperature distribution in a system, agricultural field moisture, water body thermal surface evaporation, tower cooling energy dispersion, flow in a desert cooler, and so on (Shahzad et al., 2022; Hassan et al., 2022; Salawu et al., 2022; Disu & Salawu, 2023). Sharma et al. (2012) examined diffusion-thermo and thermo-diffusion impact on the unsteady mixed convective hydromagnetic thermal radiation flow along a vertical elongated porous medium with chemically reacting species. An explicit finite numerical difference method was utilized to provide solutions to the dimensionless equations. A uniform magnetic field acts perpendicularly to the porous surface and is found to dampen the flow rate and boost the heat diffusion.

Rajashekar (2014) studied the influence of Soret and Dufour on the free convective viscous dissipation of magnetohydrodynamic porous media fluid flow in a vertically semi-indefinite surface. Various other influences have been reported including chemical reactions (Postelnicu, 2014).

In exothermic and endothermic species reactions, large quantity of heat usually accompanies reacting species process. These high thermal distributions are majorly experienced in many industrial processing systems, such as underground water pollution, fuel cell extraction, electric power generation, a chemical processing, toxic substance management and many more. In water or air, chemical reaction is observed due to the occurrence of some external masses. Hence, the study reacting species is essential in enhancing chemical technology processes such as polymer production, food processing, and ceramic and glassmare manufacturing. Das et al. (1994) considered the influence of spontaneously reacting first-order homogeneous flowing fluid through a vertical indefinite geometry with mass propagation and unvarying thermal flux. Anjalidevi and Kandasamy (2000) performed a study on the chemical reacting fluid effect on the magneto-thermal mixture of conducting liquid. Muthucumaraswamy and Genesan (2001) examined the influence of a reacting species on the impulsive, unsteady fluid flow along a vertical geometry device. Moreover, the boundary layer laminar flow of a species reacting thermal and concentration distribution has been discussed by many thermal fluidic scientists, and can be found in (Ahmed et al., 2013; Ojemen et al., 2019; Altine et al., 2020; Disu & Omokhaule, 2022).

Olanrewaju and Gbadeyan (2011) presented the effect of volumetric thermal generation/ absorption, thermal radiation, chemical reaction, Dufour and Soret on the stagnation point mixed convective streaming fluid past permeable media with an isothermal vertical surface. Dada and Adefolaju (2012) computationally examined the impacts of dissipation, magnetohydrodynamics and radiative heat on the free convective fluid flow through saturated porous media in a moving plate with thermal and species dispersion using finite difference technique. Shateyi and Motsa (2011) investigated transient convective hydromagnetic thermal and species dispersion in permeable media through a vertical boundless sheet with chemical reaction, heat radiation, thermal source/sink. Idowu et al. (2013) investigated the MHD transient flow of thermal dissipative and radiative effect on heat and mass propagation in porous vertical sheets in the existence of chemical reaction, heat generation and variable suction. Lavanya and Ratnam (2014) discussed energy and chemical species propagation effect on the free convective MHD two-dimensional flow through a permeable sheet entrenched in porous media with chemical reaction, thermal generation, heat dissipation, radiative heat, and soret and dufour impacts. Other studies on the Darcy Forchhiemer flow can be see (Hayat et al., 2016; Khan et al., 2017; Hayat et al., 2018; Rasool et al., 2021; Vedarathi et al., 2021)

Uwanta and Omokhuale (2014) employed the Crank-Nicolson finite implicit difference technique to analyze the variable heat conduction effects on Jeffery fluid, thermal and concentration distribution. Rao et al. (2015) studied the impacts of heat transfer on Jeffrey fluid on the isothermal wedge. Zhang et al. (2023) investigated Jeffrey's fluid flow of convective heating and thermal radiation. In all the studies, thermal conductivity is assumed constant despite its variation within the flow regime. Disu and Dada (2018) studied the variation of thermal conductivity on a radiative magneto-hydrodynamics flow in porous parallel wavy walls. The study revealed that temperature dependent parameters rose with increased values in the heat source.

In light of the above, it is becoming essential to study the variation of thermal conductivity in Jeffrey fluid flow. Consequently, this study aims to examine the impacts of species absorption on Jeffery fluid in saturated permeable media and variable heat conduction conductivity. The solutions to the invariant dimensionless flow model equations are obtained using a computational implicit crank-Nicolson finite difference technique. The influence diverse entrenched thermos-fluidic parameters on the fluid flow rate, thermal diffusion and mass transfer are investigated. Graphical results are offered for the parametric sensitivity of the solution outcomes; these are qualitatively presented and discussed.

Flow Model Setup

Consider a 2–dimensional transient flow of a viscous and laminar conduction Jeffery fluid in a porous, boundless, moving vertical sheet. The considered flow configuration is assumed to be in a boundless range; the dimensional physical terms are taken to be a function of t' and y', in

which y' is perpendicular to the sheet with x'-axis considered along the upward direction of the vertical surface. Without species absorption, a fluid flow injection or injection occurs on the device sheet with an imposed magnetic field on the sheet wall. The fluid maintains an initial thermal and concentration of T'_w and C'_w individually, which is considered to be more than the ambient fluid thermal energy. Moreover, the influence of chemical absorption and heat conduction variation is taken into cognizance. Assuming heat generation and viscous dissipation are not neglected while the fluid flow magnetic induction is considered negligible.

Assuming that the boundary-layer and Boussinesq approximation exist, employing the Darcy-Forchheimer model, the dynamical flow equations controlling the thermal fluid reacting species are taken as:

$$\frac{\partial v'}{\partial y'} = 0 \tag{1}$$

$$\frac{\partial u'}{\partial t'} + v'\frac{\partial u'}{\partial y'} = \frac{\nu}{1+\lambda}\frac{\partial^2 u'}{\partial y'^2} + g\beta(T' - T'_\infty) + g\beta^*(C' - C'_\infty) - \frac{\sigma B_0^2}{\rho}u' - \frac{\nu}{(1+\lambda)K^*}u' - \frac{\nu}{(1+\lambda)}\frac{b^*}{K^*}u'^2 \tag{2}$$

$$\frac{\partial T'}{\partial t'} + v'\frac{\partial T'}{\partial y'} = \frac{k_0}{\rho Cp}\frac{\partial}{\partial y'}\left\{[1 + m(T' - T'_\infty)]\frac{\partial T'}{\partial y'}\right\} + \frac{Q}{\rho Cp}(T' - T'_\infty) + \frac{\nu}{(1+\lambda)Cp}\left(\frac{\partial u'}{\partial y'}\right)^2 \tag{3}$$

$$\frac{\partial C'}{\partial t'} + v'\frac{\partial C'}{\partial y'} = D\frac{\partial^2 C'}{\partial y'^2} - R^*(C' - C'_\infty) + Q_1(T' - T'_\infty) \tag{4}$$

With the applicable initial and boundary constraints:

$$\left.\begin{array}{l} t' \le 0, u' = 0, T' \to T'_\infty, C' \to C'_\infty \; for\; all\; y' \\ t' > 0, u' = 0, \frac{\partial T'}{\partial y'} = -\frac{q}{k_0}, \frac{\partial C'}{\partial y'} = -\frac{q_m}{k_m} \;\; at\; y' = 0 \\ \quad u' \to 0, T' \to T'_\infty, C' \to C'_\infty \; as\; y' \to \infty \end{array}\right\} \tag{5}$$

where u and v denote flow rate Darcian modules in $x'$and y'axes correspondingly, t is time, T is fluid heat, g represents gravity influence, β is heat coefficient expansivity, β^* is mass coefficient expansivity, υ is viscosity, D is molecular species diffusivity, C_p is constant pressure thermal capacity, $B_0$is the intensity of the magnetic field, σ is fluid electric conduction, k_0 is varied heat conduction, $K^*$is permeability of the media, ρ is density, λ_1 is the Jeffery fluid, $b^*$is the Forchheimer term, $R^*$is reacting species term, $Q_1$is the mass absorption term, T_w is the wall temperature, $T_\infty$is the free stream temperature,$q$is heat flux,$q_m$is mass flux,$k_m$is mass diffusivity, C_w is wall concentration of the species, C_∞ is reacting species free stream, $Q$is coefficient of thermal source.

When $v_0 > 0$ denotes suction and $v_0 < 0$ represents injection. Hence, to have a dimensionless partial derivative model, the subsequent terms are introduced into the main model system of equations and their constants.

$$u = \frac{u'}{u_0}, y = \frac{u_0 y'}{\nu}, t = \frac{t' u_0}{t_0}, \nu = \frac{\mu}{\rho}, \theta = \frac{(T' - T'_\infty)k_0 u_0}{q\nu}, C = \frac{(C' - C'_\infty)k_m u_0}{q_m \nu}\Big\} \tag{6}$$

where $u_0$and $t_0$are reference velocity and time respectively.

Applying mentioned dimensionless constants and quantities on the equations (2) - (5) to get an invariant equations as:

$$\frac{\partial u}{\partial t} - \gamma\frac{\partial u}{\partial y} = \left(\frac{1}{1+\lambda}\right)\frac{\partial^2 u}{\partial y^2} + Gr\theta + GcC - Mu - \frac{1}{Da}\left(\frac{1}{1+\lambda}\right)u - \frac{Fs}{Da}\left(\frac{1}{1+\lambda}\right)u^2 \tag{7}$$

$$\frac{\partial \theta}{\partial t} - \gamma\frac{\partial \theta}{\partial y} = \frac{(1+\eta\theta)}{Pr}\frac{\partial^2 \theta}{\partial y^2} + \frac{\eta\theta}{Pr}\frac{\partial \theta}{\partial y} + S\theta + \frac{Ec}{1+\lambda}\left(\frac{\partial u}{\partial x}\right)^2 \tag{8}$$

$$\frac{\partial C}{\partial t} - \gamma\frac{\partial C}{\partial y} = \frac{1}{Sc}\frac{\partial^2 C}{\partial y^2} - RC + \phi\theta \tag{9}$$

The corresponding boundary conditions are:

$$\left.\begin{array}{l} t \le 0, u = 0, \theta = 0, C = 0 \; for \; all \; y \\ t < 0, u = 0, \frac{\partial \theta}{\partial y} = -1, \frac{\partial C}{\partial y} = -1 \;\; at \; y = 0 \\ u \to 0, \theta \to 0, C \to 0 \; as \; y \to \infty \end{array}\right\} \quad (10)$$

where

$$\left.\begin{array}{l} Pr = \frac{k_0}{\mu Cp}, M = \frac{\sigma B_0^2 \nu}{\rho {u_0}^2}, K = \frac{\nu^2}{K^* {u_0}^2}, Gr = \frac{g\beta q \nu^2}{k_0 {u_0}^4}, Gc = \frac{g\beta^* q \nu^2}{k_0 {u_0}^4} \\ Sc = \frac{\nu}{D}, Da = \frac{K^* u_9}{\nu^2}, S = \frac{Q\nu}{\rho Cp {u_0}^2}, Ec = \frac{k_0 {u_o}^2}{\rho Cpq}, Fs = \frac{b' u_0}{\nu}, \gamma = \frac{v_0}{u_0} \\ \eta = \frac{mq\nu}{k_0 u_0}, R = \frac{R^* \nu}{u_0}, \phi = \frac{Q_1 (T_w' - T_0')}{\nu (C_w' - C_0')} \end{array}\right\}.$$

Moreover $Gr$is heat convection term, Gc is concentration convection term, Pr is the Prandtl number, Sc is the Schmidt number, $M$is magnetic term, K is the permeability term, γ is the suction term, S is the heat generation term, Ec is the Eckert number. Da is Darcy term, Fs is Forchheimer term, ϕ is the mass absorption, η is a constant.

The solution to the transformed boundary value equations is obtained using of Crank-Nicolson finite implicit difference scheme. The approximation finite difference equations are as:

$$\left(\frac{u_i^{j+1} - u_i^j}{\Delta t} - \gamma \frac{u_{i+1}^j - u_i^j}{\Delta y}\right) = \frac{1}{2(1+\lambda_1)2(\Delta y)^2}\left[u_{i+1}^{j+1} - 2u_i^{j+1} + u_{i-1\;i,j}^{j+1} + u_{i+1}^j - 2u_i^j + u_{i-1}^j\right]$$

$$+ Gr\theta_i^j + GcC_i^j - Mu_i^j - \frac{1}{Da}\left(\frac{1}{1+\lambda}\right)u_i^j - \frac{Fs}{Da}\left(\frac{1}{1+\lambda}\right)u_i^j \quad (11)$$

$$\left(\frac{\theta_i^{j+1} - \theta_i^j}{\Delta t} - \gamma \frac{\theta_{i+1}^j - \theta_i^j}{\Delta y}\right) = \frac{1}{2\,Pr(\Delta y)^2}\left(1 + \frac{\eta}{2}\theta_i^j\right)\left[\theta_{i+1}^{j+1} - 2\theta_i^{j+1} + \theta_{i-1\;i,j}^{j+1} + \theta_{i+1}^j - 2\theta_i^j + \theta_{i-1}^j\right]$$

$$+ \frac{\eta}{Pr}\left(\frac{\theta_i^j - \theta_i^j}{\Delta y}\right)_i^j + S\theta_i^j + \frac{Ec}{1+\lambda}\left(\frac{u_{i+1}^j - u_i^j}{\Delta y}\right)^2 \quad (12)$$

$$\left(\frac{C_i^{j+1} - C_i^j}{\Delta t} - \gamma \frac{C_{i+1}^j - C_i^j}{\Delta y}\right) = \frac{1}{2Sc(\Delta y)^2}\left[C_{i+1}^{j+1} - C_i^{j+1} + C_{i-1\;i,j}^{j+1} + C_{i+1}^j - 2C_i^j + C_{i-1}^j\right] - RC_i^j + \phi C_i^j \quad (13)$$

The boundary and initial constraints in (10) are described as follows

$$\left.\begin{array}{l} u_{i,0} = 0, \theta_{i,0} = 0, C_{i,0} = 0 \;\; \text{for all i except } i = 0 \\ u_{i,0} = 0, \frac{\theta_{i+1,j} - \theta_{i,j}}{\Delta y} = -1, \frac{C_{i+1,j} - C_{i,j}}{\Delta y} = -1 \\ u_{L,0} = 0, \theta_{L,0} = 0, C_{L,0} = 0 \end{array}\right. \quad (14)$$

where L agrees to infinity. The suffix i satisfies to j and y is equivalent to t. accordingly, $\Delta t = t_{j+1} - t_j$and $\Delta y = y_{i+1} - y_i$.

Numerical Procedure

Computed results for the flow rate dispersion u, thermal distribution θ and mass transfer C are graphically exhibited to enhance the perception of the physical problems. These results are presented via computed values of solutant Grashof number, Schmidt number, suction term, magnetic term, Prandtl number, Jeffery term, heat Grashof number, Darcy number, Forchheimer term, mass absorption, porosity term, thermal source term, viscous term on the flow rate, heat

dispersion and species transfer. The solutions are obtained via a Crank-Nicolson finite implicit difference procedure. This scheme is unconditionally convergent and stable. All calculations are done using the values for Gr = Gc = M =η = S = 1,$\lambda_1 = \phi = 0.5$, Pr = 0.71, Sc = 0.6, Ec = 0.2, Da = Fs = 0.5, K= 0.5, $\gamma = 0.5$ except as presented in each graph. A step size of ΔY = 0.001 is utilized in the range Y_{min}= 0 to Y_{max}= 5 for a favorite precision and a convergence criterion of 10^{-6} is gratified for diverse terms.

Results and Discussion

For the outputs C, θ, u at time t, the time $t + \Delta t$ value is gotten for $i = 1,2,\ldots,L-1$ in equation (13). The results for θ and u are from the equations (11) and (12). This technique is continuous to have a suitable solution outcome at time t.

Velocity Distribution

Figures 1 to 14 illustrate the velocity distribution for the variation of terms individually. Figure 1 displays the influence of the Prandtl number on the fluid flow rate. The Jeffrey fluid flow rate reduces as the Prandtl number increases. The decline in the flow velocity is due to the enhanced viscosity and molecular bonding that restricted free flow. Also, the heat source and fluid particle interaction are discouraged, which opposes the flow rate; This thereby declines the velocity field of the Jeffery fluid. Figure 2 reveals the impact of varying Hartmann term M values on the velocity distribution. The non-Newtonian velocity field declines with an increase in the magnetic term. An increase in the magnetic field induced electromagnetic force to create a Lorentz force that opposes the free flow of the fluid velocity and, in turn, decreases the velocity distribution. Figure 3 portrays a variation in the Schmidt number about the velocity field. The term Sc estimates the effectiveness relation between mass transfer and momentum diffusivity. Hence, the velocity boundary film declines with a reduced number of Sc. Figure 4 investigates the effect of the term Darcy Da on the momentum dimension. The flow velocity dimension is encouraged as the Da value increases. The higher the medium pore, the higher the flow rate of the Jeffery fluid.

Figure 5 illustrates the influence of the Jeffery term on the flow velocity profile. An increase in the Jeffery term values stimulates a rising flow velocity along the porous media because internal heating reduces the fluid viscosity. The velovity gradient is inspired as the momentum boundary gets thinner for an enhanced convective heat transfer, which consequently weakens the molecular bonding and results in the rising velocity distribution of jeffery fluid. Figure 6 demonstrates the influence of increasing thermal generation on the velocity distribution. As obtained in the plot, the flow velocity profile significantly increased with increasing heat generation values along the flow regime. Fluid particle collision and interaction propel the strengthening of current-carrying fluid heat dispersion, thereby increasing the velocity profile as depicted. Meanwhile, Figure 7 confirms the impact-enhancing suction term on the Jeffery fluid flow rate. It is realized from the flow dimension that the non-Newtonian flow velocity field is well pronounced due to the rising suction term, which encouraged internal heating, viscous dissipation and reaction species distribution.

Figures 8 and 9 represent the diverse effects of increasing the values of the thermal convection and solutal convection parameters on the flow velocity profiles. It is noticed from the flow behavior that the velocity is boosted with upsurging thermal and solutal convection terms. The buoyancy force encourages Jeffery liquid particle interaction, thereby stimulating the fluid velocity field. Thus, the momentum boundary film viscosity is prompted as the Gr or Gc parameter values are enhanced. The impact of strengthening the values of the term Fs on the velocity profile is exhibited in Figure 10. As noticed from the flow dimension, a significant damp in the velocity field is obtained with respect to an increase in the numbers of Fs. Figure 11 shows the velocity profile's response to the chemical reaction's rising effect. The flow velocity is damped as the viscosity and molecular boding force are stimulated to restrict the velocity field. Figure 12 shows the velocity profile's response to the chemical reaction's rising effect. Figure 13 demonstrates the

impact of the variational rise in the Eckert number with the flow velocity distribution. Boosting the Eckert number has been shown to promote the velocity profile by enhancing thermal dissipation, thereby increasing the flow rate. Figure 14 gives the influence of the parameter ϕ on the fluid flow dimensional regime. The plot shows that increasing the parameter ϕ values boosts the velocity profile. The behavior is due to the enhanced boundary layer thickness that encouraged thermal conduction and conveciton with the system, thereby enhancing the velocity distribution of the fluid.

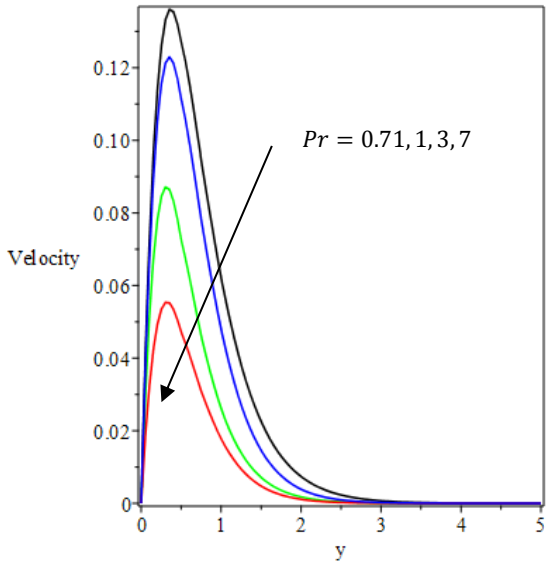

Figure 1. Flow rate with diverse values of the term Pr

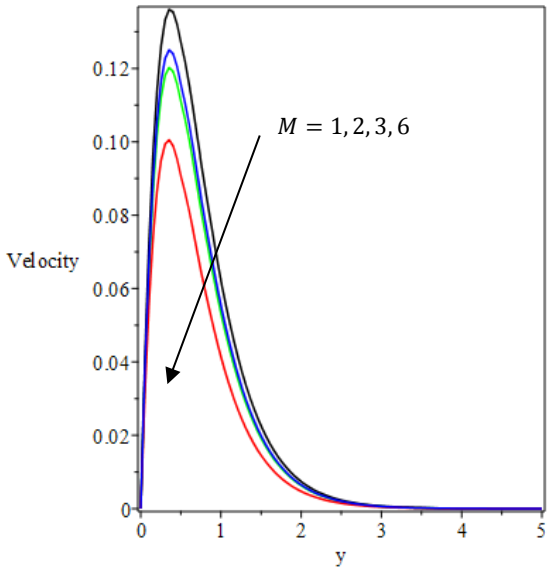

Figure 2. Velocity distribution for an increasing values M

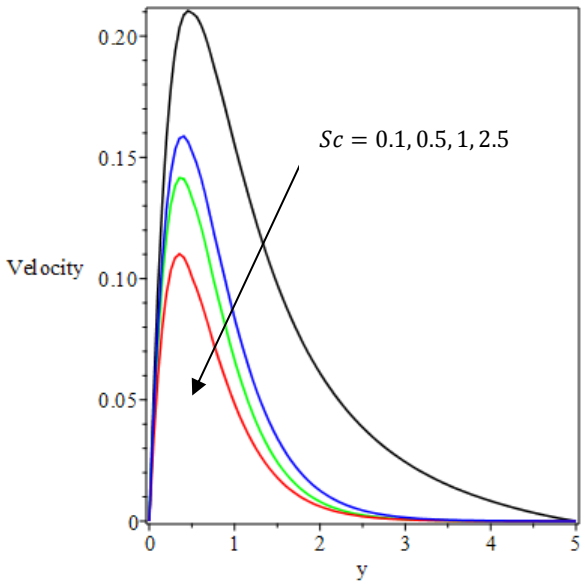

Figure 3. The rising Sc values effect on the velocity field

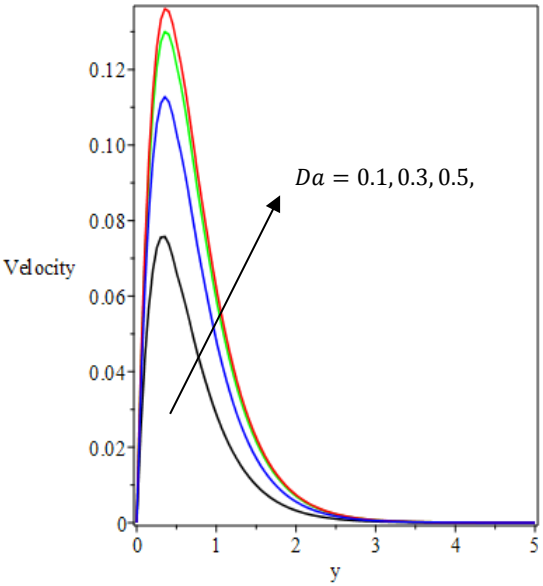

Figure 4. Flow rate field for variation in Da values

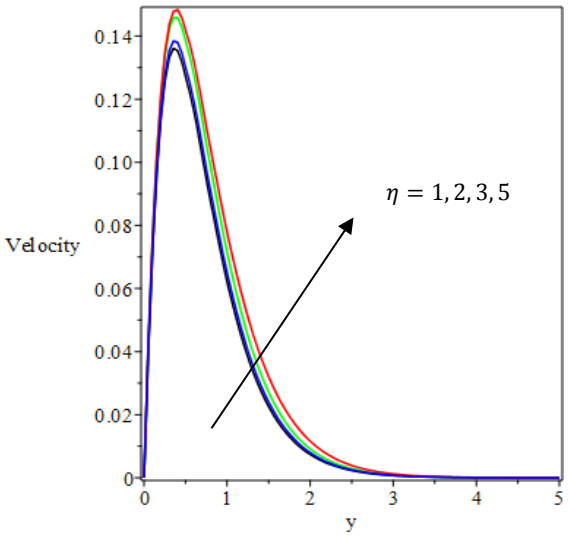

Figure 5. The response of flow velocity to enhancing values of η

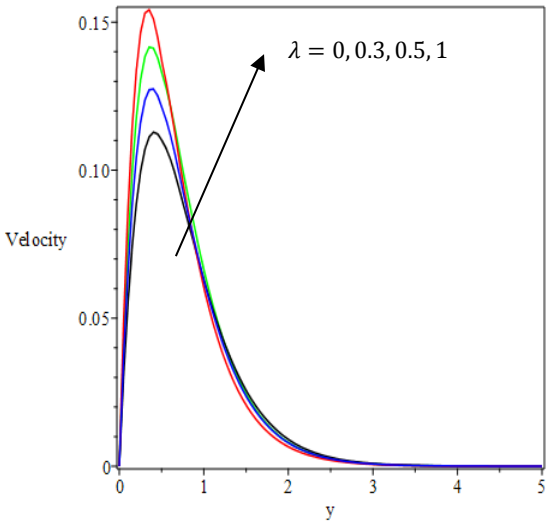

Figure 6. The reaction of flow velocity field to various numbers of λ

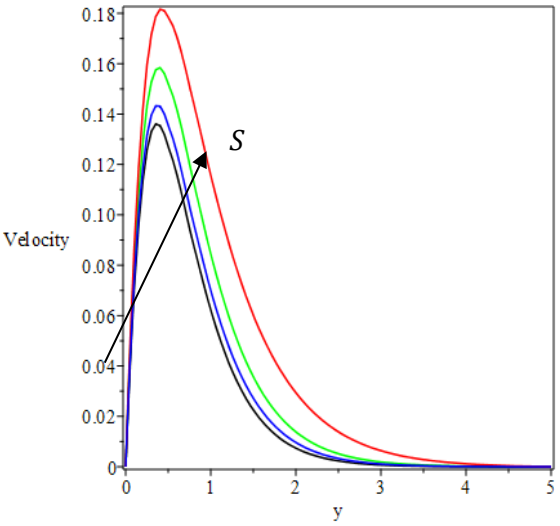

Figure 7. Velocity field in response to an increased term S.

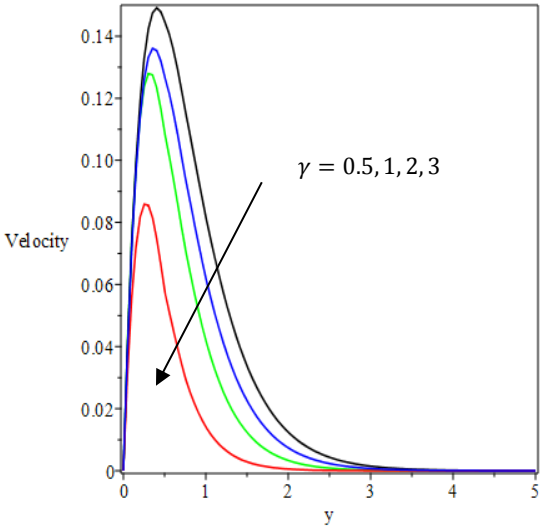

Figure 8. Flow dimension for increasing values of γ

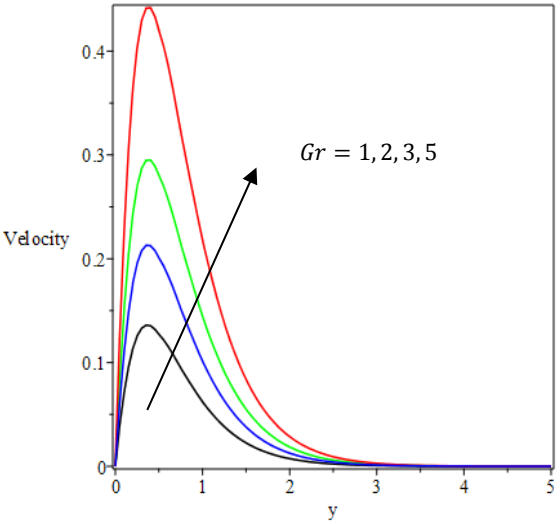

Figure 9. Influence of rising values of Gr on the velocity profile

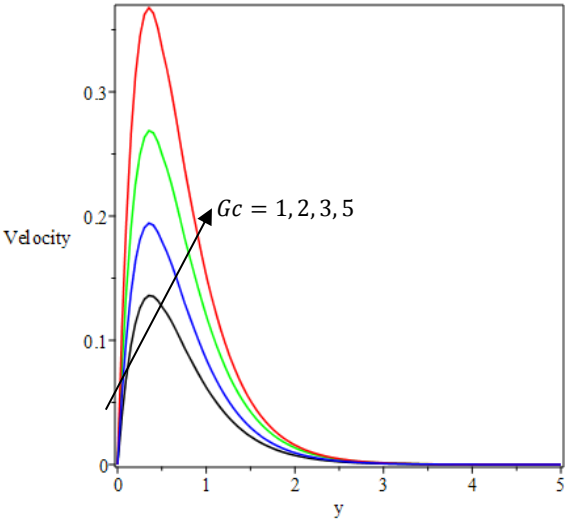

Figure 10. The impact of boosting the values of Gc on the flow rate.

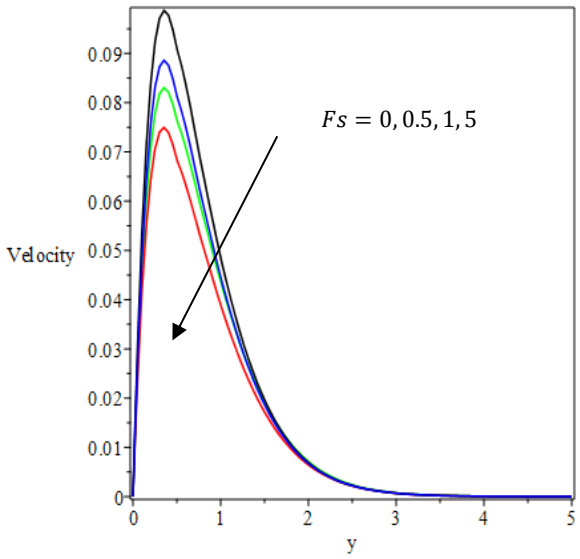

Figure 11. Effect of raising the number Fs on the velocity field

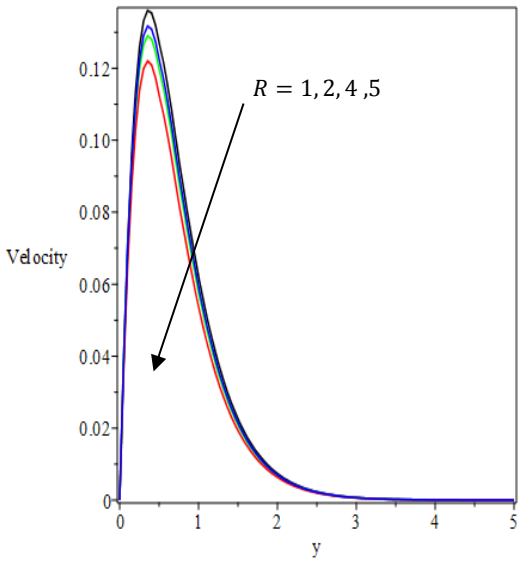

Figure 12. The effect of increasing R values on the velocity profile

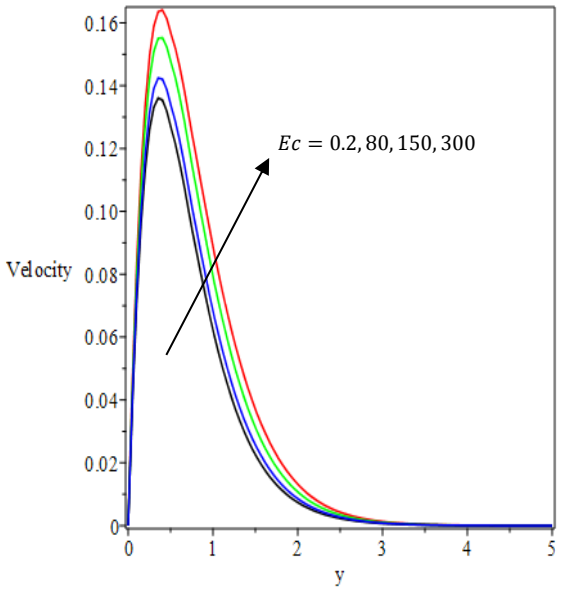

Figure 13. The response of the velocity field to a rising values Ec

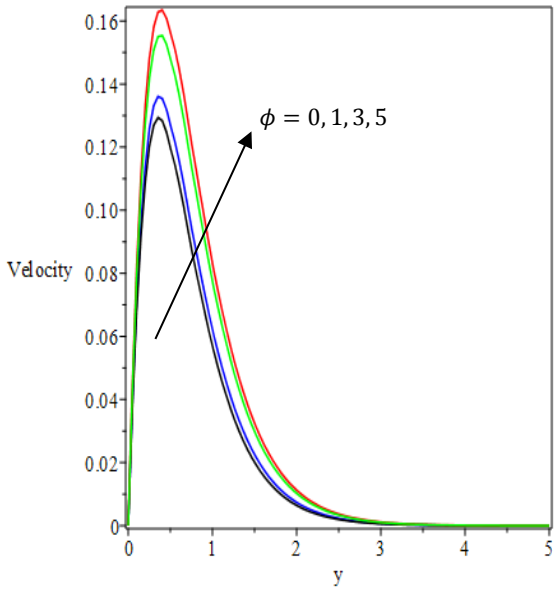

Figure 14. The impact of the term ϕ on the flow rate filed

Thermal distributions

Figures 15 to 20 represent the thermal distributions. In Figure 15, the Prandtl number influence on the thermal dispersion in a boundless boundary layer is depicted in the plot. The plot demonstrates that the thermal distribution declines as the Prandtl number is raised. The cause of the observation is that lower numbers of Pr correspond to a momentous rise in the fluid heat conduction. Therefore, high thermal diffusion occurs through the heated plate speedily for lower numbers of Pr than higher numbers. Thus, lower Prandtl values enhanced the heat boundary film thickness, which leads to a reduced thermal transfer. Figure 16 demonstrates the response of the temperature distribution to an increasing heat source. This confirmed that the heat propagation is raised as the thermal generation within the system is boosted. A variational rise in the effect of the wall suction term on heat diffusion is exhibited in Figure 17. The dimensional thermal regime depicted that the heat dispersion is decreased as the values of the suction term are augmented. Moreover, Figure 18 portrays the consequence flow stream constant η on the Jeffery thermal particle migration. As the plot offers, the temperature field increases along the thermal region

far stream with rising constant values. As seen in Figure 19, the viscous heating term induces heat generation in the system, which prompts the temperature profile. Therefore, the rising Eckert number significantly spurs internal heating and fluid particle migration, thus enhancing the heat field. Figure 20 displays the effect of disparity time relation to the temperature circulation in the boundless configuration system. As time increasingly varies, the overall heat generation and temperature distribution is raised as depicted in the plot.

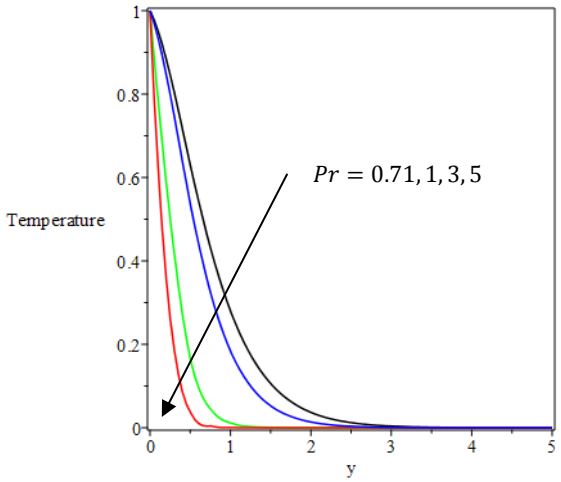

Figure 15. Thermal field with dissimilar Pr numbers

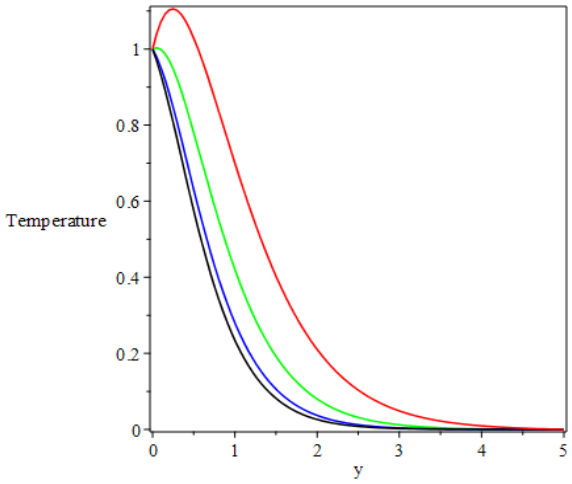

Figure 16. Temperature field versus increasing values of S

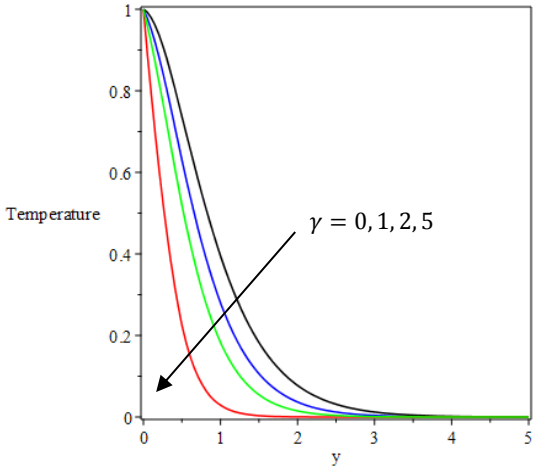

Figure 17. Heat propagation with variational rise in γ values.

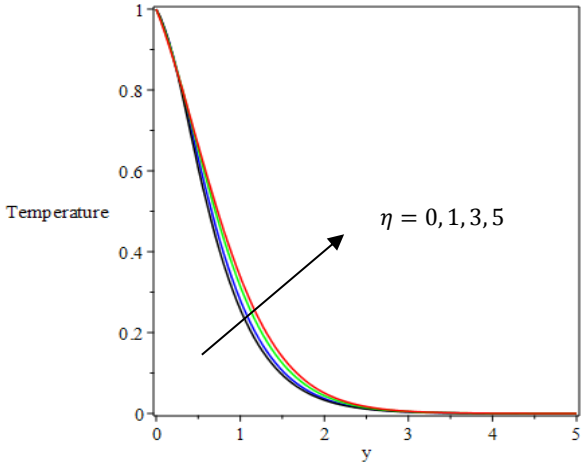

Figure 18. Thermal dispersion field for diverse numbers of η

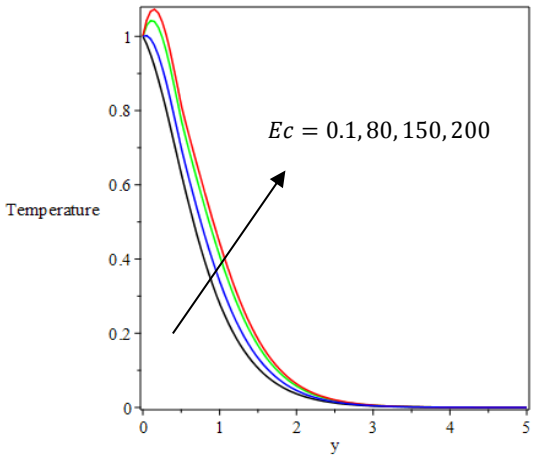

Figure 19. Temperature dispersion with rising values of Ec

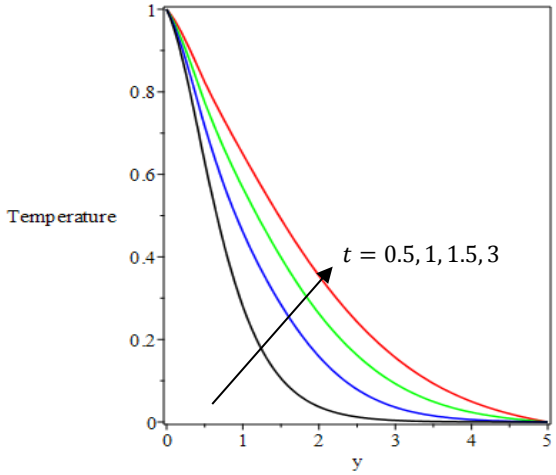

Figure 20. Heat distribution for variation in time t

Concentration Distribution

Figures 21 to 25 display the species' mass diffusion field. The increasing Schmidt numbers impact the species mass distribution, as obtainable in Figure 21. The graph indicates that increasing Schmidt numbers momentously discouraged the species concentration profile. This is due to the dominance of the mass buoyancy force over the chemical reacting Jeffery fluid. Internal heating and reaction activation energy is damped, reducing mass transfer magnitude. Declination in the mass transfer profile is convoyed simultaneously to reduce the flow rate and mass diffusion boundary film. Figure 22 presents the influence of varying suction terms on the chemical reacting species field. It is noticed from the flow behavior that the Jeffery concentration distribution declines for an augmenting suction term. However, Figure 23 confirms the impression of the chemical reacting term on the mass distribution. The graph shows that the concentration field is damped with increasing chemical reacting term. Figure 24 shows that the species' mass reaction and distribution are enhanced with a variational raised in the distinction time. Figure 25 describes the influence of the parameter ϕ on the mass transfer. It is shown that the species particle diffusion increased as the values of the term ϕ were raised.

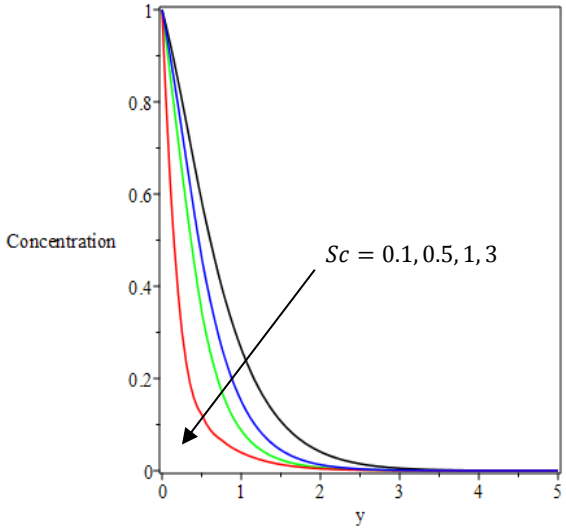

Figure 21. Mass transfer for increasing Sc numbers

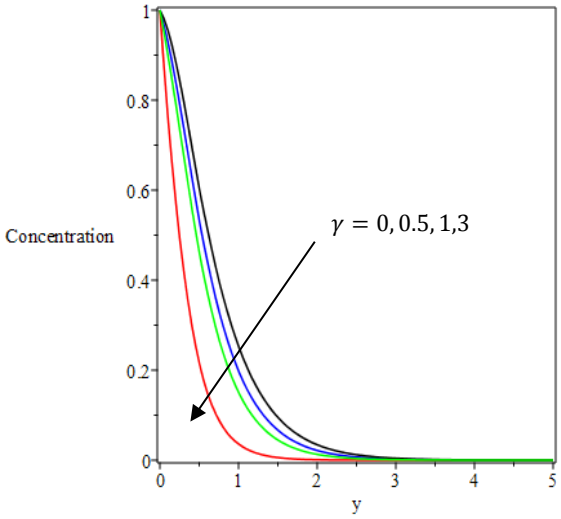

Figure 22. Reacting species distribution with rising values of γ

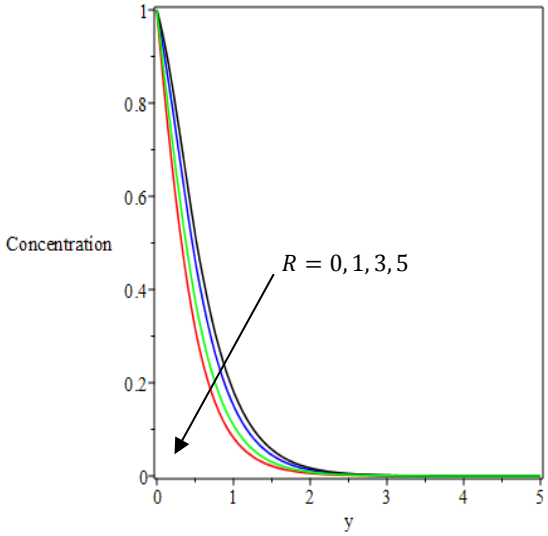

Figure 23. Concentration distribution with variation in the R values

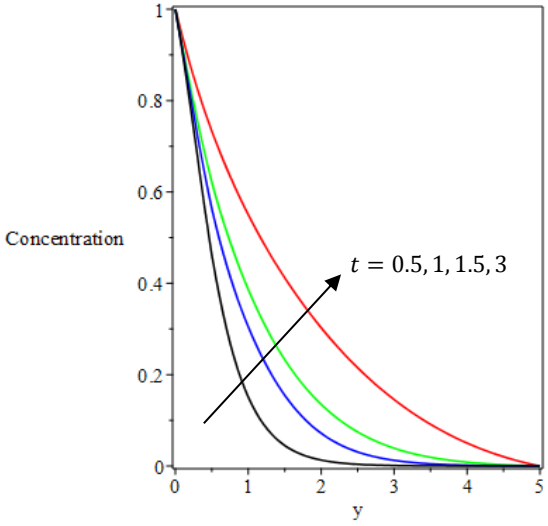

Figure 24. Effect of variational boost in time t on the concentration field

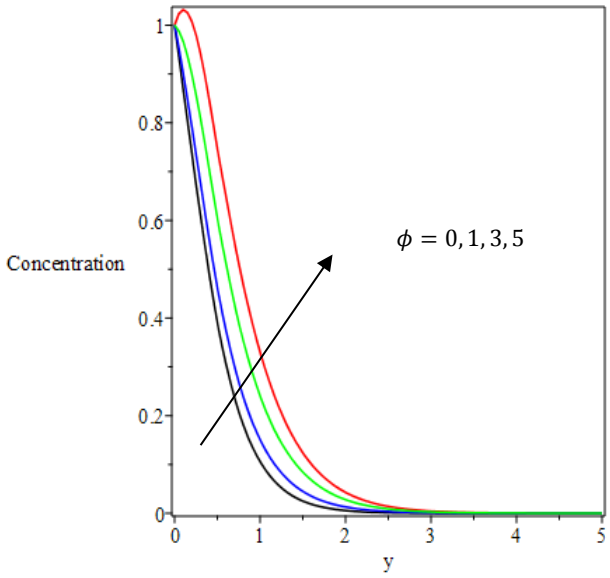

Figure 25. The impact of the term ϕ on the mass distribution.

Conclusion

The research investigation examines the effect of chemical absorption of Jeffery liquid with variable heat conduction in saturated permeable media. From the computation analysis and solutions of the modeled equations, the resulting conclusion can be drawn:

- The presence of a chemically reactive species significantly alters the flow dynamics of Jeffery fluid in porous media. The absorption of the chemical species into the fluid modifies the viscosity and elasticity of the fluid which, in turn, affects the flow characteristics.
- Variable thermal conductivity profoundly impacts heat transfer within the fluid regions, leading to temperature gradients that influence fluid viscosity and flow patterns.
- The porosity and permeability of the medium affect the distribution and movement of the fluid, as well as the dispersion and absorption of the chemical species.

The finding can help design a more efficient system by optimizing fluid flow and heat transfer properties according to specific operational requirements. The study underscores the intricate relationship between chemical absorption, thermal conductivity, and fluid flow in porous media. It achieves a more comprehensive understanding of Jeffery's fluid dynamics in such environments, paving the way for improved design and optimization in practical application.

Acknowledgments

The authors appreciate and acknowledge the reviewers' contribution in making the article robust.

Conflicts of interest

The authors declare that there are no conflicts of interest.

References

Ahmed, N., Gaswami, J. K., & Barua, D. P. (2013). Effects of chemical reaction and radiation on an unsteady MHD flow past an accelerated infinite vertical plate with variable temperature and mass transfer. Indian Journal of Pure and Applied Mathematics, 44(4), 443 – 466.

Altine, M. M., Omokhaule, O., Onwubuya, I. O. & Disu A. B. (2020). Heat absorption effect on free convection flow past vertical porous pipe with mass transfer. International Journal of Science for Global Sustainability, 6(1), 94-100.

Anjalidevi, S. P. & Kandasamy, R. (2000). Effects of chemical reaction heat and mass transfer on MHD flow past aa semi-infinite plate. Z. Angew. Mathematics and Mechanics, 80, 697-701.

Dada, M. S. & Adefolaju, F. H. (2012). Dissipation, MHD and radiation effects on an unsteady convective heat and mass transfer in a Darcy-Forchheimer porous medium. Journal of Mathematics Research, 4(2), 110 – 127.

Das, U. N., Deka, R. K. & Soundalgekar, V. M. (1994). Effects of mass Transfer on flow past an impulsively stated infinite vertical plate with constant heat flux and chemical reaction. Forsch. Ingenieurwes, 60, 284 – 287.

Disu, A. B. & Dada M. S. (2018). Effects of variable thermal conductivity on radiative MHD flow in a porous medium between two vertical wavy walls. Scientia Africana: An International Journal of Pure and Applied Sciences Volume 17(1), 89 -102

Disu, A. B. & Omokhuale E. (2022). Effects of injection and Heat sink/source on convective Kuvshink fluid through a porous medium. Communication in Physical Sciences, 8(2), 145-157.

Disu, A. B. & Salawu, S. 0. (2023). Thermal distribution of magneto-tangent hyperbolic flowing fluid over a porous sheet: A lie-group analysis. Journal of Nigerian Society of Physical Sciences 5(2023)1103.

Hassan, A.R., Salawu, S .O., Disu, A. B. & Aderele, O. R., (2022). Thermodynamic analysis of a tangent hyperbolic hydromagnetic heat generating fluid in quadratic Boussinesq approximation. Journal of Computational Mathematics and Data Science, 4, 100058.

Hayat, T., Muhammad, T., Saleh, A. & Liao, S. (2016). Darcy-Forchhiemer flow with variable thermal conductivity and catta-neo-christov heat flux. International Journal of Numerical Methods for Heat Fluid Flow, 28(8):2355 – 2369.

Hayat, T., Shah, F., Hussain, Z. & Alseadi, A. (2018). Darcy Forchheimer flow of Jeffery Nanofluid with heat generation/absorption and melting heat transfer. Thermal Science, 23, 314-314.

Idowu, A. S., Dada, M. S., and Jimoh, A. (2013). Heat and mass transfer of magnetohydrodynamics (Mhd) and dissipative fluid flow past a vertical moving plate with variable suction. Mathematics Theory and Modelling, 3(3), 80 – 102.

Lavanya, B. and Ratman, A. L. (2014). Dufour and Soret effects on steady MHD free convective flow past a vertical porous plate embedded in a porous medium with chemical reaction, radiation, heat generation and viscous dissipation. Advances in Applied Science Research, 5(1), 127 – 142.

Kandasamy, R., Periasamy, K. & Sivagnana Prabhu, K. K. (2005). Effects of chemical reactions heat and mass transfer along a wedge with heat source in the presence of suction/injection. International Journal of Heat Mass Transfer, 48, 1388 – 1393.

Khan, M. I., Hayat, T. & Alsaedi, A. (2017). Numerical analysis for Darcy-Forchhiemer flow in presence of homogeneous-heterogeneous reactions, Results in Physics, 7, 2644-2650.

Muthucumaraswamy, R. & Ganesan, P. (2001). First order chemical reaction on flow past an impulsively stated vertical plate with uniform heat and mass flux. Acta Mehanica, 147, 45 – 57.

Ojemen G., Disu A. B. & Omokhauale E. (2019). Combination effects of radiative heat source and magnetic field on a free convective flow in moving vertical plate filled with porous material. Caliphate Journal of Science and Technology, 2(1), 135-140.

Olanrewaju, P. O. & Gbadeyan, J. A. (2011). Effects of Soret, Dufour and chemical reaction, thermal radiation and volumetric heat generation/absorption on mixed convection stagnation point flow on an isothermal vertical plate in a porous media. Pacific Journal of Science and Technology, 12(2), 234 – 245.

Postelnicu, A. (2007). Influence of chemical reaction on heat and mass transfer by natural Convection from vertical surfaces in a porous media considering Soret and Dufour effects. Heat and Mass Transfer, 43, 595 – 602.

Rajashekar, M. N. (2014). Effects of Dufour and Soret on unsteady MHD heat and mass transfer flow past a semi-infinite moving vertical plate in a porous medium with viscous dissipation. International Journal op Applied Physics and Mathematics, 4(2), 130 – 134.

Rao A. S., Nagenda N. & Prasad V. R. (2015). Heat transfer in a non-Newtonian Jeffery's fluid over non-isothermal wedge. International Conference on Computational Heat and Mass Transfer, 127, 775-782.

Rasool, G., Shafiq, A. & Durur, H. (2021). Darcy-Forchhiemer relation in magnetohydrodynamic Jeffery nanofluid over stretching surface. Discrete and Continuous Dynamical Systems Series S, 14(7), 2497 – 2515.

Sharma, B. K., Yadav, K., Mishra, N. K., & Chaudhary, R. C. (2012). Soret and Dufour effects on unsteady MHD mixed convection flow past a radiative vertical porous plate embedded in a porous medium with chemical reaction. Applied Mathematics, 3, 717- 723.

Shahzad, F., Jamshed, W., Sajid, T., Shamshuddin, M. D., Safdar, R., Salawu, S. O., Eid, M.R., Hafeez, M. B. & Krawczuk, M. (2022). Electromagnetic control and dynamics of generalized Burgers nanoliquid flow containing motile microorganisms with Cattaneo-Christov relations: Galerkin finite element mechanism. Applied Sciences, 12(17), 8636.

Salawu**,** S.O., Obalalu, A. M. & Shamshuddin, M. D. (2022). Nonlinear solar thermal radiation efficiency and energy optimization for magnetized hybrid Prandtl-Eyring nanoliquid in aircraft. Arabian Journal for Science and engineering, 22, 070801.

Sharma, B. K., Yadav, K., Mishra, N. K. & Chaudhary, R. C. (2012). Soret and Dufour effects on unsteady MHD mixed convection flow past a radiative vertical porous plate embedded in a porous medium with chemical reaction. Applied Mathematics, 3, 717- 723.

Shateyi, S. and Motsa, S. (2011). Unsteady Magnetohydrodynamics convective heat and mass transfer past an infinite vertical plate in a porous medium with thermal radiation, heat generation/absorption and chemical reaction. Advance Topics in Mass Transfer, 7, 145 – 162.

Uwanta. I. J. & Omokhuale, E. (2014). Effects of variable thermal conductivity on heat and mass transfer with Jeffery fluid. International Journal of Mathematical Archive, 5(3). 135 – 149.

Vedarathi, N., Dharmaiah, G., Venkatadri, K. & Gaffar, S. A. (2021). Numerical Study of radiative non-darcy nanofluid flow over a stretching sheet with a convective conditions and energy activation. Nonlinear Engineering, 10: 159 – 176.

Zhang R., Zaydan M., Alshehri M., Raju C.S.K., Wakif A. & Shah N. A. (2023). Further insights into mixed convective boundary layer flows of internally heating Jeffrey nano-fluids: Stefan's blowing case study with connective heating and thermal radiation. Case Study in Thermal Engineering, 104121.